A Novel Prognostic Signature for Hepatocellular Carcinoma Based on Sumoylation-Related Genes

Jianping Wang
Qingdao Municipal Hospital
Peipei Cong
Qingdao Municipal Hospital
Zhipeng Jin
Qingdao Municipal Hospital
Lingli Liu
Qingdao Municipal Hospital
Dongxu Sun
Qingdao Municipal Hospital
Wenjing Zhu
Qingdao Municipal Hospital
Guangjun Shi (sgjzp@hotmail.com)
Qingdao Municipal Hospital

Article

Keywords: Hepatocellular carcinoma, SUMOylation-related genes, Prognostic model, Immunocytes, Drug sensitivity.

Posted Date: March 21st, 2022

DOI: https://doi.org/10.21203/rs.3.rs-1442809/v1

Version of Record: A version of this preprint was published at Scientific Reports on July 11th, 2023. See the published version at https://doi.org/10.1038/s41598-023-38197-4.

Abstract

SUMOylation (SUMO modification) has been confirmed to play an important role in the progression of various malignancies. As the value of SUMOylation-related genes (SRGs) in prognosis prediction of hepatocellular carcinoma (HCC) has not been explored, we aimed to construct a HCC SRGs signature. RNA sequencing was utilized to identify differentially expressed SRGs. The 87 identified genes were used in Univariate Cox regression analysis and the Least Absolute Shrinkage and Selection Operator (LASSO) analysis to build a signature. The signature was prognostic in the TCGA and ICGC datasets. The GSEA revealed that the risk score was also associated with common cancer-related pathways. The ssGSEA showed NK cells in the high-risk group was significantly reduced. The sensitivities of anti-cancer drugs confirmed the sensitivity of the high-risk group to sorafenib was lower. Further, Our cohort showed that risk scores were correlated with advanced grade and Vascular invasion (VI). Finally, the results of H&E staining and immunohistochemistry of Ki67 showed that higher-risk patients are more malignant.

Introduction

Hepatocellular carcinoma (HCC) is one of the most common diagnosed cancer types worldwide [1]. This severe disease, which accounts for more than 75% of the primary liver cancer cases, has high mortality and is typically developed from chronic hepatitis and cirrhosis [2–3]. Despite the enormous advances achieved in diagnostic techniques, the overall survival period of patients with HCC is shorter due to late disease identification and diagnosis [4]. Over the years, traditional treatments for HCC patients showed poor clinical effect [5]. VI is a significant factor affecting prognosis in HCC [6]. Another study also reported that patients with VI, compared to those without evidence of VI, showed a shorter median survival [7]. Hence, VI was included in our study as an important clinical indicator.

SUMOylation is a protein modification pathway that regulates various biological processes, including cell division, signal transduction, DNA repair, and cell metabolism [8]. SUMOylation consists of a three-step enzymatic reaction, including activation, coupling, and ligation [9]. Accumulating evidence has shown that many cancers have significantly enhanced SUMOylation dynamics [10]. Thus, SUMOylation can be viewed as a global mechanism that increases the stability and robustness of complex signaling pathways, which, if unchecked or spuriously activated, can exert disastrous consequences for cells [11]. The abnormal expression of SUMOylation might be a cause of tumor progression and could thus serve as a novel marker [12]. Currently, due to the ease of access of public databases, a growing number of signatures have been discovered that predict the patients' prognosis, whereas no SUMOylation-related risk signature has been identified in HCC patients.

In the present research, we screened out SRGs related with prognosis in HCC, analyzed the TCGA database by Lasso Cox regression to develop a model. Moreover, the predictive accuracy of the risk feature was tested in a ICGC cohort and our cohort. The research might provide a new method for clinical treatment of HCC.

Results

Identification of HCC prognosis-associated DEGs

We obtained the expression data of the mRNA sequences of 50 normal tissue and 374 HCC tissue samples by searching the TCGA database. Differentially expressed SRGs in tumor and normal samples were filtrated by the limma package in R (|logFC| > 1.0, FDR < 0.05). Finally, 2 and 85 SRGs were significantly down-regulated and up-regulated, respectively. The information of these findings is displayed in the heat-map, depicted in Fig. 2a. Thirty-five SRGs were tested to be closely related to HCC prognosis by univariate Cox regression analysis (Fig. 2b).

Construction of a SRGs-based prognostic model

Subsequently, the 35 genes were analyzed by Lasso regression analysis for building a risk signature. The signature consisted of the following two genes: *CDCA8* and *CBX2*, and regression coefficients. This prognostic signature was developed to calculate the risk score by the following formula: Risk score = (0.03166 × expression of *CDCA8*) + (0.40426 × expression of *CBX2*). Then, based on the median risk score, HCC patients were divided into two groups in the TCGA cohort: high-risk (n = 146) and the low-risk (n = 146). We used Kaplan–Meier curves to compare the difference in the overall survival between two groups. The high-risk HCC patients, compared to the low-risk group, had a clearly worse 5-year survival probability ($P < 0.05$).(Fig. 3a) Afterwards, we constructed a heat map, showing the expression levels of two genes in different groups of patients. (Fig. 3b) Patient's survival time was presented as a scatter plot, and the risk scores were ranked in an ascending order, revealing that the high-risk patients had a worse prognosis (Fig. 3c, d) Further research showed that the mRNA expression in the two model genes in normal tissue was significantly lower than that in the tumor tissue samples. (Fig. 3e) In addition, the high expression levels of the two SRGs indicated a low survival rate in the K-M curve. (Fig. 3f) Finally, the genetic alterations of two genes from 366 HCC samples analyzed in the cBioPortal database revealed the existence of mutations in 24 patients (6.5%) (Fig. 3g).

Evaluating the Prognostic Value

Initially, the two model genes expression and clinical characters was shown on the heatmap. (Fig. 4a) Then, univariate Cox regression analyses demonstrated that age, stage and risk score could predict the prognosis of HCC patients. Risk score and stage were found to be independent prognostic factors ($P < 0.05$, HR > 1) by multivariate Cox regression analysis. (Fig. 4b) Furthermore, the time-dependent ROC curves revealed that AUC values of 1-, 2-, and 3-year in the TCGA cohort were 0.723, 0.647, and 0.642, respectively. These results suggested that the prognostic model was effective in accurately predicting the survival time (Fig. 4c). To assess the clinical significance, we developed multifactor ROC curves, which showed that the risk score (AUC: 0.713) was better for predicting the survival time of HCC patients than those of other clinical factors (Fig. 4d).

Validation of the prediction ability by the ICGC database

We utilized the ICGC cohort to validate the accuracy of the prognostic signature. First, the expression levels of two genes in the tumor tissues were found to be also higher than in the normal tissues (Fig. 5a). Next, based on the computational formula in the TCGA database, the HCC patients in the ICGC database were also divided into two sets (Fig. 5b). The results showed that the patients in the low-risk group had a better survival time (Fig. 5c). The univariate and multivariate analyses suggested that risk score and stage could be used as independent indexes for prognosis prediction (Fig. 5d). In addition, the AUC values of the time-dependent ROC curves (1-, 2-, and 3-year) were 0.760, 0.745, and 0.774, correspondingly, which showed that the risk signature met the criteria for prognosis prediction (Fig. 5e).

Correlations between the risk model and the clinical factors

The association between risk score and clinical factors was explored. Our results showed that the risk score (Fig. S1a) were related to the grade, stage, and VI of patients. The patients with advanced stage, higher grade and VI had higher risk score in TCGA. Meanwhile, the risk score were related to the stage in ICGC (Fig. S1b).

Nomogram construction

To apply the prognostic model for the prediction of the survival time of HCC patients, we further combined the age, stage with the risk score to build the 1-, 2-, and 3-year OS prediction nomograms. Based on the nomogram, we could build an average patient score to determine patients' OS (Fig. S2a). In addition, the calibration diagrams indicated that the nomogram had an excellent performance (Fig. S2b).

Pathways correlated with the risk score

To explore the signaling pathway underlying the SRGs model, we conducted GSEA. The results revealed that SUMOylation and several common tumor-related pathways, such as cell cycle, neurotrophin signaling pathway, pathways in cancer, base excision repair, MAPK, VEGF and P53 signaling pathway, were significantly enriched in the high-risk patients. (Fig. S3)

Correlation between the prognostic model and tumor immune micro-environment

The ssGSEA showed that patients with high-risk score had a significantly higher level of immune cell infiltration including Macrophages, aDCs, Tfh, Treg, Th2 cells, but lower proportions of Natural killer (NK) cells (Fig. S4a). Interestingly, immune-related functional pathways, such as the score of Type-II IFN response, CCR, Check point, MHC class I, APC co stimulation, were different between the low- and high-risk group in the TCGA cohort (Fig S4b). In ICGC cohort, the ssGSEA demonstrated the result of immune cell infifiltration (e.g., B cells, Neutrophils, NK cells and Th2 cells) and immune-related functional pathways (e.g., Type-I IFN Response and Type-II IFN Response) (Fig. S4c, d). In conclusion, NK cells and Type-II IFN Response of high- and low-risk had statistically significant differences in TCGA and ICGC.

Drug susceptibility analysis

Eight common chemotherapy drugs were selected to analyze to examine the sensitivity of different risk groups to chemotherapy. We analyzed that the high-risk patients scores had lower IC50 values for paclitaxel, gemcitabine, doxorubicin, bleomycin (Fig. 6a), whereas the IC50 values of chemotherapeutics, such as sorafenib, gefitinib, docetaxel, and AKT inhibitor VIII were significantly lower in the patients with low risk scores (Fig. 6b). To sum up, the aforementioned results showed that the risk scores were associated to drug sensitivity.

Verification of clinical tissue samples

Further, we validated the accuracy of the signature in our cohort from Qingdao Municipal Hospital. First, we standardized the expression level and obtained the risk score by the formula: Risk score = (0.03166 × relative expression of *CDCA8*) + (0.40426 × relative expression of *CBX2*). The median risk score was utilized as a cut-off value to classify patients into a high-risk (n = 5) or a low-risk group (n = 5). The risk scores of these ten patients and their clinical information are listed in **table.3**. Next, we analyzed the relationship between the risk scores and clinical factors, which displayed that the risk score was associated with vascular invasion and tumor grade by fisher Chi-square tests (**Table 4**). And, results of H&E staining and immunohistochemistry in sample 1, 2 and sample 9, 10 are exhibited in Fig. 7.

Discussion

HCC is a deadly disease with a very low 5-year survival rate [20]. Therefore, it is critically important to build a reliable and effective prognostic model for patients with HCC. Numerous medical studies in the past have shown that SUMOylation is closely related to tumorigenesis, metastasis, and proliferation and is significantly upregulated in most tumors [21, 22]. Hence, SUMOylation could be a potential target for future cancer discoveries and therapy. Nevertheless, the gene expression of SUMOylation in HCC is still not well understood.

In this study, we first screened 187 DEGs in TCGA cohort. We analyzed the relationship between DEGs and HCC patients' prognosis by univariate Cox analysis. Then, we used LASSO regression analysis to develop a two-gene SUMOylation-related prognostic model in the TCGA database and tested its accuracy using the ICGC database. Patients in TCGA and ICGC were divided into high- and low-risk groups. Further, we found that the high-risk patients had a worse prognosis compared with the low-risk patients. Finally, risk score was an independent prognostic factor in the TCGA and ICGC cohorts, which was verified by multivariate analysis. Finally, we estimated the performance of the risk model in the following aspects: clinical characteristics, GSEA, tumor immune micro-environment, and chemotherapeutic susceptibility to several drugs. The aforementioned results revealed that this prognostic signature had good clinical guidance significance and could be used to predict patient prognosis.

The risk model included two genes (*CDCA8* and *CBX2*). Two genes were over-expressed in HCC tissues, which was associated with a low survival rate. The previous study had demonstrated HCC cell progression was inhibited by knockdown of CDCA8. This process was achieved by restoring ATF3 tumor suppressor and restraining AKT signaling pathway [23]. Molecular targeted therapy of *CDCA8* might be an effective systemic approach to prevent tumor recurrence by eliminating cancer stem cells and cancer cells. [24]. CBX (Chromobox Homolog 2) in the PRC1 complex SUMOylates CETN2 at an unknown residue with SUMO2,3 [25]. The knockdown of *CBX2* expression in HCC cells increased HCC cell apoptosis, suppresses HCC cell proliferation. [26]

We constructed a risk model to provide further, more effective guidance of clinical diagnosis and treatment. Our study showed that the high-risk group were correlated with vascular invasion, advanced stage and higher grade. In present study, vascular invasion was a very important clinical index.[27] Both micro-invasion and macro-invasion were correlate with tumor poor survival [28]. We found that high-risk groups was more likely to develop the vascular invasion in TCGA and our cohort. This results could guild the clinical works. For instance, high-risk groups need early surgical treatment to prevent vascular invasion. In addition, high-risk patients were more possible to experience tumor recurrence.

The GSEA indicated that a high-risk score was significantly associated with some common HCC potential pathways (e.g., SUMOylaton, neurotrophin signaling pathway, cell cycle and so on). And the association of most of these pathways with the occurrence and therapy of HCC has been previously validated. For example, it was becoming clear that cancers exhibited substantially enhanced SUMOylation dynamics [10]. Loss of normal cell cycle control was an important beginning of tumor. Cancer cells accumulate alterations leading to unscheduled proliferation and genomic instability.[29] Mesencephalic astrocyte-derived neurotrophic factor (MANF) levels were associated with the status of liver cirrhosis, advanced stage, and tumor size. [30] We forecast that the activation of these pathways might be the reason of high-risk patients with the poor survival.

In recent studies, the application of immune micro-environment has been used as a novel anti-cancer therapy [31]. The results of NK cell and IFN response II had statistical significance in our study. NK cell was a main anti-tumor cell in the liver, and which could affect other immune cells' anti-tumor behavior. [32]. Previous studies had observed that the SUMOylation inhibitor enhanced the proportions of activated NK cells in vivo treatment [33]. The results showed that the immune infiltration of NK cells in the high-risk group was significantly reduced, which could explain the reason of high-risk group with the poor prognosis. IFN response plays crucial roles in promoting host anti-tumor immunity and is considered to be pivotal components in the cancer-elimination phase of the cancer immunosurveillance. [34]

In this study, the sensitivity of the high-risk group to sorafenib was lower than that of the low-risk, whereas higher gemcitabine sensitivity was observed in the high-risk patients. Therefore, high-risk patients resistant to sorafenib can be treated with gemcitabine, which may achieve better results.

According to the risk signature, we chose the highest risk score of clinical sample (sample 1, 2) and the lowest risk score (sample 9, 10). Moreover, the results of H&E staining and immunohistochemistry of Ki67

confirmed that patients with high risk score are more malignant.

We developed a SRGs-related risk model and tested the accuracy of risk model using a number of approaches. Subsequently, we further explored the possible mechanism and pathways involved. Certainly, the risk model had limitations. First, only external cohorts and the Qingdao Municipal Hospital cohort (only 10 samples) were included in this study. Second, no further functional in vivo or in vitro experiments were conducted to reveal the potential mechanisms of the gene model.

Materials And Methods

The flow chart was presented in Fig. 1.

Patients and HCC specimens

HCC tissues were acquired from 10 HCC patients who received operation at Qingdao Municipal Hospital (Qingdao, Shandong, China) in 2020, which were frozen for western blotting. Meanwhile, clinical information of each patient was documented in detail. Each patient signed informed consent. The research had been approved by the Ethics Committee of Qingdao Municipal Hospital. All assays were consistent with the Declaration of Helsinki regulations.

RNA extraction and qRT-PCR

After tissue grinding, total RNA was extracted with TRIzol reagent (Tiangen, China). cDNAs were obtained from total RNAs by using PrimeScript RT reagent Kit (TaKaRa, Japan). The realtime PCR (qRT-PCR) experiment was performed using TB Green Premix Ex Taq II (TaKaRa, Japan). The expression levels were normalized with GAPDH. The primer sequences used in this study are displayed in Table 1.

Table 1
Primer sequences for two genes and GAPDH

Primer name	Primer sequence
CDCA8 forward	AGCAGGACAGTTGGCAGCAG
CDCA8 reverse	AGTCCCACTGACCACCTCCC
CBX2 forward	GCGGCTGGTCCTCCAAACAT
CBX2 reverse	TGGCAGTGAGCTTCCTTGGC
GAPDH forward	GACCTGACCTGCCGTCTA
GAPDH reverse	AGGAGTGGGTGTCGCTGT

Table.2 The clinical characteristic information of the HCC patients in TCGA and ICGC.

Characteristics	TCGA (%)	ICGC (%)
Age		
< 65	176 (60.27)	81 (35.53)
≥ 65	116 (39.73)	147 (64.47)
Gender		
Male	194 (66.44)	NA
Female	98 (33.56)	NA
Survival status		
Alive	205 (70.21)	185 (81.14)
Dead	87(29.79)	43(18.86)
Stage		
Stage I&II	232 (79.45)	141 (61.84)
Stage III&IV	60 (20.55)	87 (38.16)
Histological grade		
G1-2	177 (60.62)	NA
G3-4	115 (39.38)	NA
Vascular invasion		
None	192 (65.75)	NA
Micro or Macro	100 (34.25)	NA

Data acquisition

We downloaded the data of the mRNA expression and the clinical information of the included HCC patients from the TCGA database (https://cancergenome.nih.gov/) and ICGC database (http://dcc.icgc.org) (Table 2). Duplicate and missing data in two databases were deleted. A total number of 187 SUMOylation-related genes were downloaded by gene sets “REACTOME_SUMOYLATION” from the GSEA website (https://www.gsea-msigdb.org) [13]. The data downloaded from TCGA and ICGC databases was freely publicly available.

DEG screening and prognostic signature establishment

First, we evaluated the differentially expressed SRGs from the TCGA database by the “limma” package in R software 3.6.2 [14], based on the following standard: |log2 Fold Change |> 1.0 and FDR < 0.05. Next,

univariate Cox analysis was utilized to determine the prognostic SRGs. Lasso was employed to develop a formula using the “glmnet” package in R software. The survival time of the high- and low-risk groups was established by Kaplan– Meier curve construction. Finally, we conducted research on the cBioPortal (http://cbioportal .org) to obtain data on the genetic alterations of the genes of the HCC patients [15].

Signature accuracy validation

First, univariate and multivariate Cox analyses were employed to validate the independent prognostic value of risk score. Next, time-dependent receiver operating characteristic (ROC) curve analysis was applied to evaluate the accuracy of the signature by the “timeROC” package [16]. C-index value > 0.6 was considered to have acceptable predictive value. The multi-factor ROC was utilized for comparisons of the prognostic superior values of the signature and important clinical factors, such as gender, age, stage, grade and VI. Finally, the accuracy of this model was assessed in a ICGC cohort.

Nomogram construction

Recently, nomograms have been extensively utilized to predict the survival time. In this study, we first, we used the “rms” package in R to establish a nomogram based on the signature and clinical factors to predict patients’ overall survival. Then, calibration curves were developed to evaluate the accuracy of the nomogram.

Relationship between the SRGs model and the clinical features

The “ggpubr” package was utilized to determine the relationship between the risk score and clinical factors, including the stage, grade, and VI in HCC patients.

GSEA

To explore the enriched pathways associated with our model, Gene set enrichment analysis (GSEA) was performed using GSEA 4.2.1 software [17]. FDR < 0.05 was considered to indicate statistical significance.

Association between the signature and immunocytes

We further employed the single-sample gene set enrichment analysis (ssGSEA) in the "gsva" package to assess the difference of 16 immune cells and 13 immune-related pathways in high- and low-risk groups [18].

Drug sensitivity prediction

The half-maximal inhibitory concentration (IC50) was applied to explore the association between the risk score and anti-cancer drugs. The IC50 of each HCC sample was predicted using the pRRophetic package [19] in R.

Statistical analysis

The statistical analysis was used by R software (4.0.2) and Perl language packages. A K-M curve was used to compare the overall survival time of the different groups via the log-rank test. The comparisons between the two groups were analyzed by Wilcoxon rank-sum test. Spearman correlation and fisher Chi-square tests were performed to measure the correlation between variables. $P < 0.05$ indicated statistically significant differences.

Table.3 Clinical parameters of 10 HCC from clinical patients.

Sample	Grade	stage	VI	risk score	risk
1	G3	Stage III	invasion	0.43592	high
2	G3	Stage II	invasion	0.378746328	high
3	G4	Stage III	invasion	0.148692076	high
4	G3	Stage II	invasion	0.14270414	high
5	G3	Stage I	invasion	0.114524725	high
6	G2	Stage I	no	0.088184136	low
7	G3	Stage I	no	0.083630926	low
8	G2	Stage IV	invasion	0.07453907	low
9	G2	Stage IV	no	0.07453907	low
10	G1	Stage I	no	0.058986327	low

Table.4 The fisher Chi-square tests.

Characteristics		risk		P value
		high	low	
Grade	1-2	0	4	0.0238
	3-4	5	1	
Stage	I&II	3	3	1
	III&IV	2	2	
VI	no	0	4	0.0238
	invasion	5	1	

Declarations

ACKNOWLEDGMENTS

Grant from Qingdao Municipal Key Research Development Program (2020-WJZD) are gratefully acknowledged. The authors would also like to thank Journal Experts for proofreading the article.

AUTHOR CONTRIBUTIONS STATEMENT

Jianping Wang and Zhipeng Jin designed the experiments; Lingli Liu and Wenjing Zhu analyzed and interpreted the data. Dongxu Sun and Peipei Cong performed the experiments; Jianping Wang and Guangjun Shi wrote the manuscript. All the authors revised the manuscript.

CONFLICTS OF INTEREST

The authors declare that there are no conflicts of interest.

Ethics declarations

All methods were carried out in accordance with relevant guidelines and regulations.

Data availability

The datasets analysed during the current study are available in public, open access repositories listed in this article.

References

1. Sung Hyuna,Ferlay Jacques,Siegel Rebecca L et al. Global cancer statistics 2020: GLOBOCAN estimates of incidence and mortality worldwide for 36 cancers in 185 countries.[J] .CA Cancer J Clin, 2021, undefined: undefined.

2. Ryu T, Takami Y, Wada Y, Hara T, Sasaki S, Saitsu H. Actual 10-year survival after surgical microwave ablation for hepatocellular carcinoma: a single center experience in Japan. Ann Surg Oncol. 2019;26(12):4126–33.

3. Zheng J, Kuk D, Gönen M, Balachandran VP, Kingham TP, Allen PJ, D'Angelica MI, Jarnagin WR, DeMatteo RP. Actual 10-year survivors after resection of hepatocellular carcinoma. Ann Surg Oncol. 2017; 24(5):1358–66.

4. Forner Alejandro,Reig María,Bruix Jordi,Hepatocellular carcinoma.[J] .Lancet, 2018, 391: 1301-1314.

5. Xie, Y. et al. Immunotherapy for hepatocellular carcinoma: Current advances and future expectations. J. Immunol. Res. 2018, 8740976 (2018).

6. Shah SA, Cleary SP, Wei AC, et al. Recurrence after liver resection for hepatocellular carcinoma: risk factors, treatment, and outcomes. Surgery. 2007;141:330–339.

7. Pawlik TM, Poon RT, Abdalla EK, et al. Critical appraisal of the clinical and pathologic predictors of survival after resection of large hepatocellular carcinoma. Arch Surg. 2005;140:450–458.

8. Chang Hui-Ming,Yeh Edward T H,SUMO: From Bench to Bedside.[J] .Physiol Rev, 2020, 100: 1599-1619.

9. Gareau JR, Lima CD. The SUMO pathway: emerging mechanisms that shape specificity, conjugation and recognition. Nat Rev Mol Cell Biol 2010;11:861-71.

10. Seeler Jacob-Sebastian,Dejean Anne,SUMO and the robustness of cancer.[J] .Nat Rev Cancer, 2017, 17: 184-197.

11. Seeler Jacob-Sebastian,Dejean Anne,SUMO and the robustness of cancer.[J] .Nat Rev Cancer, 2017, 17: 184-197.

12. Boulanger M, Paolillo R, Piechaczyk M, et al. The SUMO Pathway in Hematomalignancies and Their Response to Therapies. Int J Mol Sci 2019;20:3895.

13. Subramanian Aravind,Tamayo Pablo,Mootha Vamsi K et al. Gene set enrichment analysis: a knowledge-based approach for interpreting genome-wide expression profiles.[J] .Proc Natl Acad Sci U S A, 2005, 102: 15545-50.

14. Ritchie Matthew E,Phipson Belinda,Wu Di et al. limma powers differential expression analyses for RNA-sequencing and microarray studies.[J] .Nucleic Acids Res, 2015, 43: e47.

15. Cerami Ethan,Gao Jianjiong,Dogrusoz Ugur et al. The cBio cancer genomics portal: an open platform for exploring multidimensional cancer genomics data.[J] .Cancer Discov, 2012, 2

16. C. Combescure, T. V. Perneger, D. C. Weber, J. P. Daurès, and Y. Foucher, “Prognostic ROC curves a method for representing the overall discriminative capacity of binary markers with right-censored time-to-event endpoints,” Epidemiology, vol. 25, no. 1, pp. 103–109, 2014

17. Subramanian Aravind,Tamayo Pablo,Mootha Vamsi K et al. Gene set enrichment analysis: a knowledge-based approach for interpreting genome-wide expression profiles.[J] .Proc Natl Acad Sci U S A, 2005, 102: 15545-50.

18. Rooney MS, Shukla SA, Wu CJ, et al. Molecular and genetic properties of tumors associated with local immune cytolytic activity. Cell. 2015;160(1–2):48–61. doi: 10.1016/j.cell.2014.12.033.

19. Geeleher Paul,Cox Nancy,Huang R Stephanie,pRRophetic: an R package for prediction of clinical chemotherapeutic response from tumor gene expression levels.[J] .PLoS One, 2014, 9: e107468.

20. Bray F, Ferlay J, Soerjomataram I, Siegel RL, Torre LA, Jemal A. Global cancer statistics 2018: GLOBOCAN estimates of incidence and mortality worldwide for 36 cancers in 185 countries. Cancer J Clin. 2018;68(6):394–424.

21. Human Protein Atlas Bogachek Maria V,Park Jung M,De Andrade James P et al. Inhibiting the SUMO Pathway Represses the Cancer Stem Cell Population in Breast and Colorectal Carcinomas.[J] .Stem Cell Reports, 2016, 7: 1140-1151.

22. He Xingyue,Riceberg Jessica,Soucy Teresa et al. Probing the roles of SUMOylation in cancer cell biology by using a selective SAE inhibitor.[J] .Nat Chem Biol, 2017, 13: 1164-1171.

23. Jeon Taewon,Ko Min Ji,Seo Yu-Ri et al. Silencing CDCA8 Suppresses Hepatocellular Carcinoma Growth and Stemness via Restoration of ATF3 Tumor Suppressor and Inactivation of AKT/β-Catenin Signaling.[J] .Cancers (Basel), 2021, 13: undefined.

24. Jeon Taewon,Ko Min Ji,Seo Yu-Ri et al. Silencing CDCA8 Suppresses Hepatocellular Carcinoma Growth and Stemness via Restoration of ATF3 Tumor Suppressor and Inactivation of AKT/β-Catenin Signaling.[J] .Cancers (Basel), 2021, 13: undefined.

25. Klein Ulf R,Nigg Erich A,SUMO-dependent regulation of centrin-2.[J] .J Cell Sci, 2009, 122: 3312-21.

26. Mao Jiakai,Tian Yu,Wang Chengye et al. CBX2 Regulates Proliferation and Apoptosis via the Phosphorylation of YAP in Hepatocellular Carcinoma.[J] .J Cancer, 2019, 10: 2706-2719.

27. Hsieh Chen-Hsi,Wei Chang-Kuo,Yin Wen-Yao et al. Vascular invasion affects survival in early hepatocellular carcinoma.[J] .Mol Clin Oncol, 2015, 3: 252-256.

28. Sumie Shuji,Nakashima Osamu,Okuda Koji et al. The significance of classifying microvascular invasion in patients with hepatocellular carcinoma.[J] .Ann Surg Oncol, 2014, 21: 1002-9.

29. Dominguez-Brauer Carmen,Thu Kelsie L,Mason Jacqueline M et al. Targeting Mitosis in Cancer: Emerging Strategies.[J] .Mol Cell, 2015, 60: 524-36.

30. Liu Jun,Wu Zhengsheng,Han Dan et al. Mesencephalic Astrocyte-Derived Neurotrophic Factor Inhibits Liver Cancer Through Small Ubiquitin-Related Modifier (SUMO)ylation-Related Suppression of NF-κB/Snail Signaling Pathway and Epithelial-Mesenchymal Transition.[J] .Hepatology, 2020, 71: 1262-1278.

31. Justus CR, Sanderlin EJ, Yang LV. Molecularconnections between cancer cell metabolism and the tumor micro-environment. Int J Mol Sci. 2015;16(5):11055–11086.

32. Vivier E, Ugolini S, Blaise D, Chabannon C, Brossay L. Targeting natural killer cells and natural killer T cells in cancer. Nat Rev Immunol. 2012;12(4):239-252. Published 2012 Mar 22. doi:10.1038/nri3174.

33. Kumar S, Schoonderwoerd MJA, Kroonen JS, de Graaf IJ, Sluijter M, Ruano D, González-Prieto R, Verlaan-de Vries M, Rip J, Arens R, de Miranda NFCC, Hawinkels LJAC, van Hall T, Vertegaal ACO. Targeting pancreatic cancer by TAK-981: a SUMOylation inhibitor that activates the immune system and blocks cancer cell cycle progression in a preclinical model. Gut. 2022 Jan 24:gutjnl-2021-324834. doi: 10.1136/gutjnl-2021-324834. Epub ahead of print. PMID: 35074907.

34. Dunn GP, Koebel CM, Schreiber RD. Interferons, immunity and cancer immunoediting. Nat Rev Immunol. 2006;6(11):836-848. doi:10.1038/nri1961

Figures

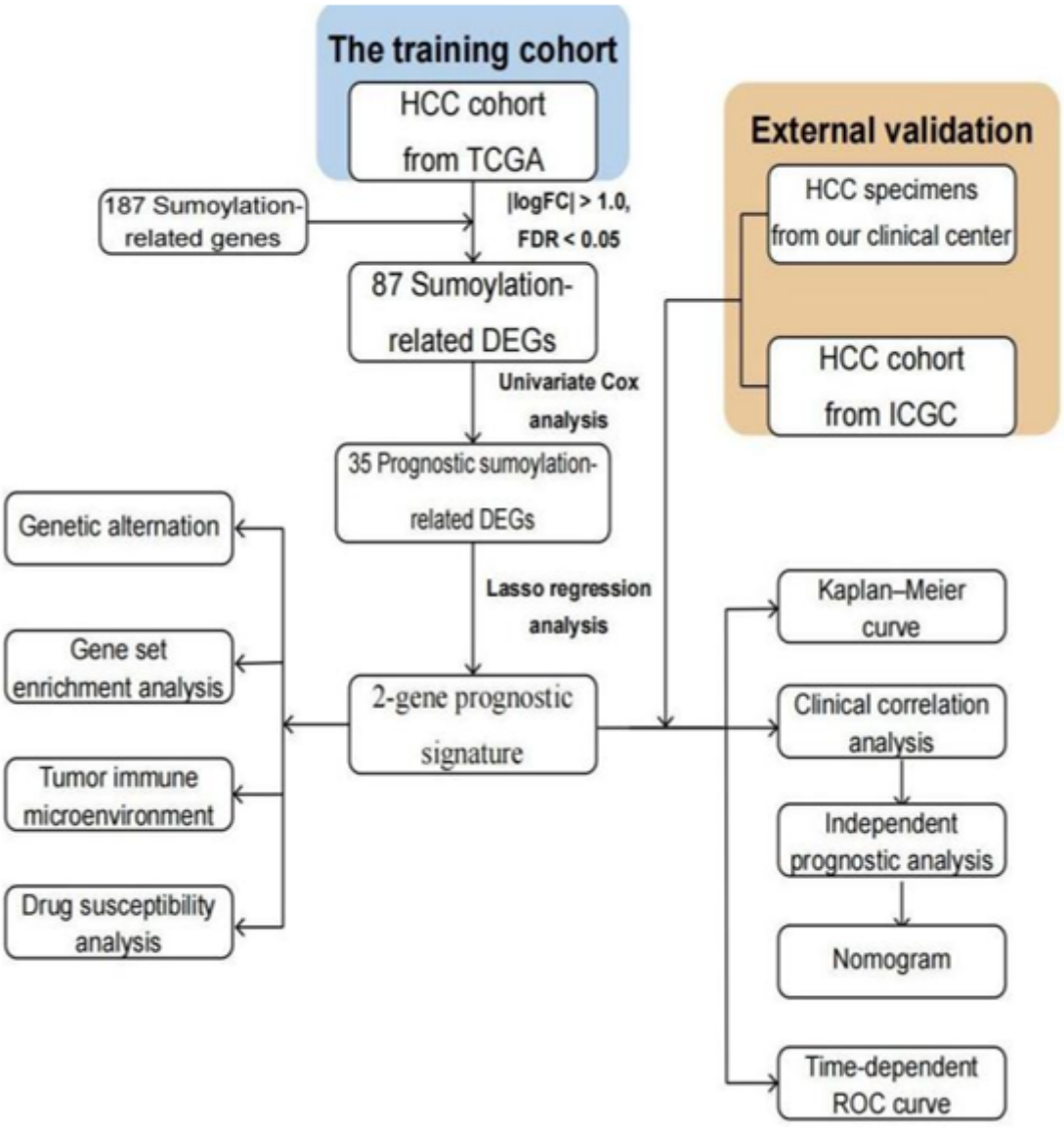

Figure 1

The flow chart.

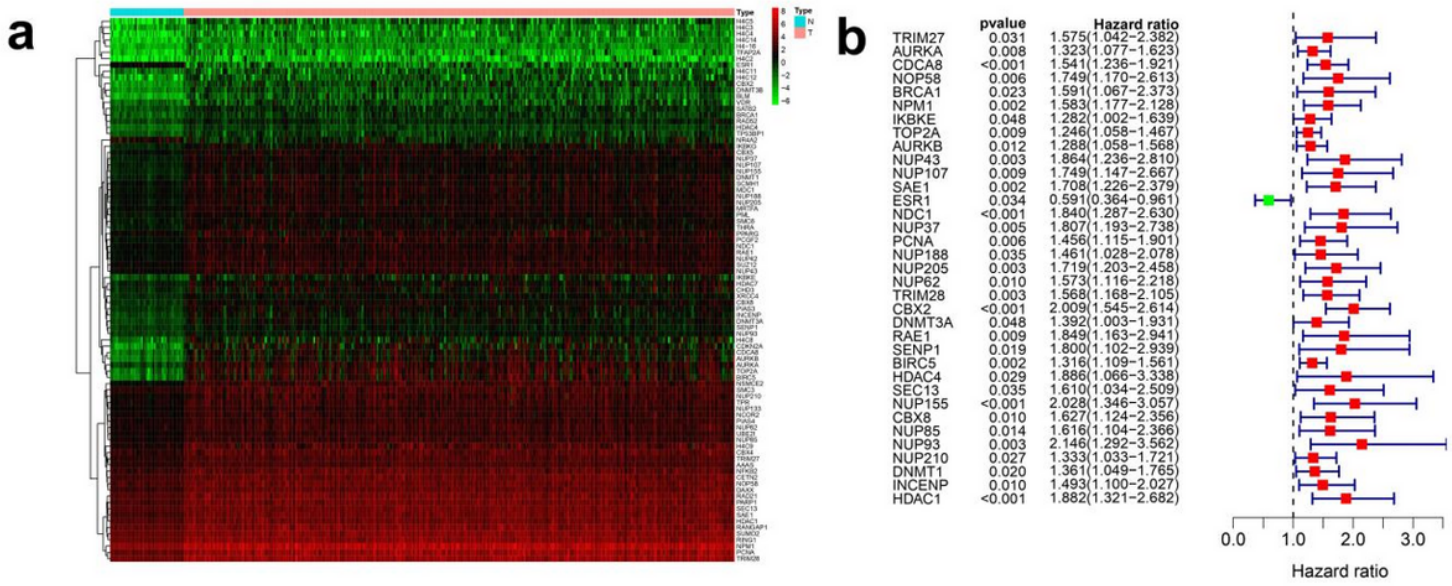

Figure 2

Identification of HCC prognosis related DEGs. (a) Heatmap of the 87 identified SRGs; (b) Forest plot of the univariate Cox regression results.

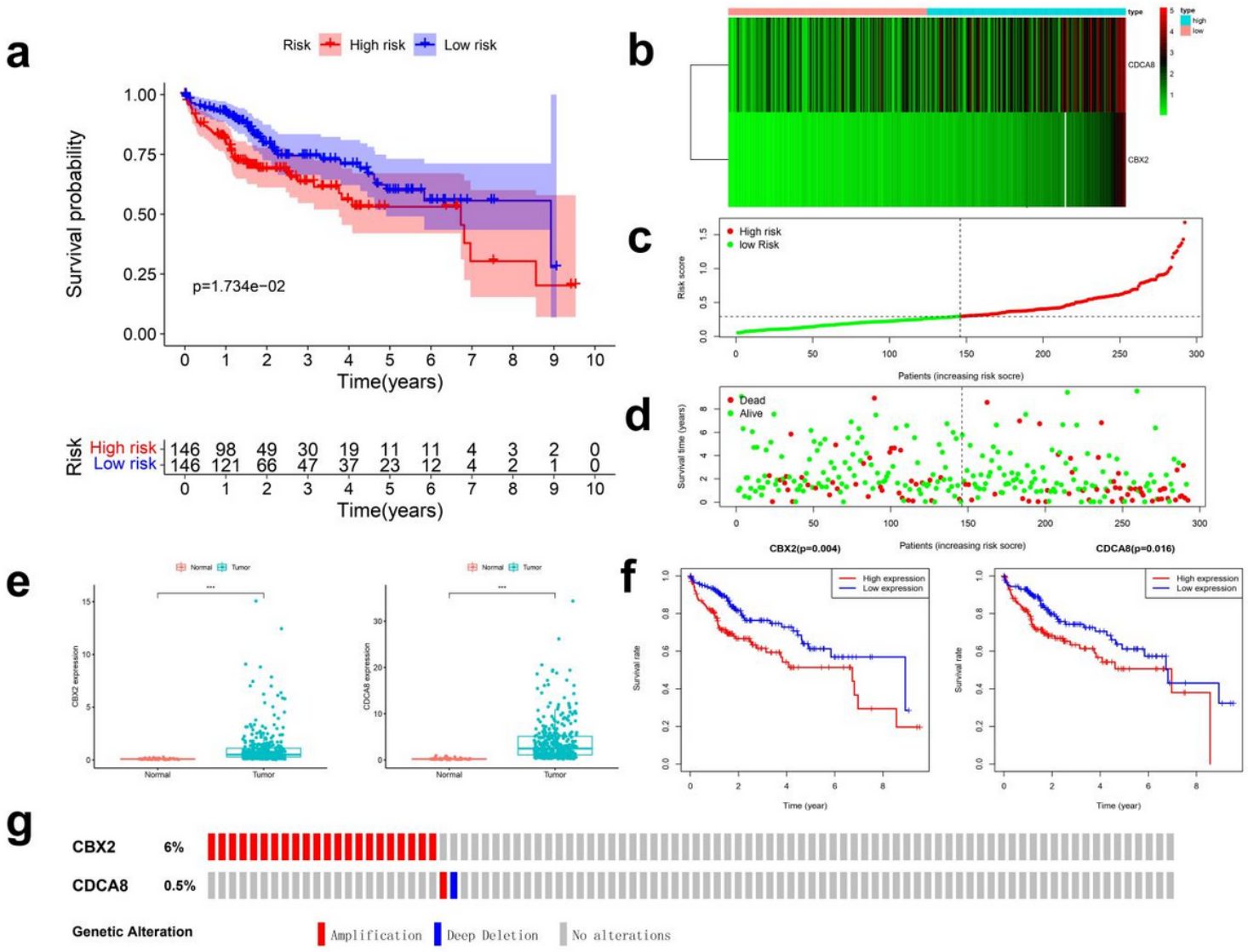

Figure 3

Construction of a prognostic model. (a) The patients in the low-risk groups have significantly longer OS outcomes than those in the high-risk groups; (b) Expression heatmap of two prognostic SRGs in high- and low-risk groups; (c) Risk score distribution in HCC patients; (d) Overall survival and survival status of HCC patients in the TCGA database; (e) Expression levels of two screened SRGs in HCC and normal samples; (f) K-M curve of the relationship between OS in HCC patients and expression levels; (g) Mutation data of two screened SRGs among 366 HCC specimens according to the data derived from the cBioPortal database.

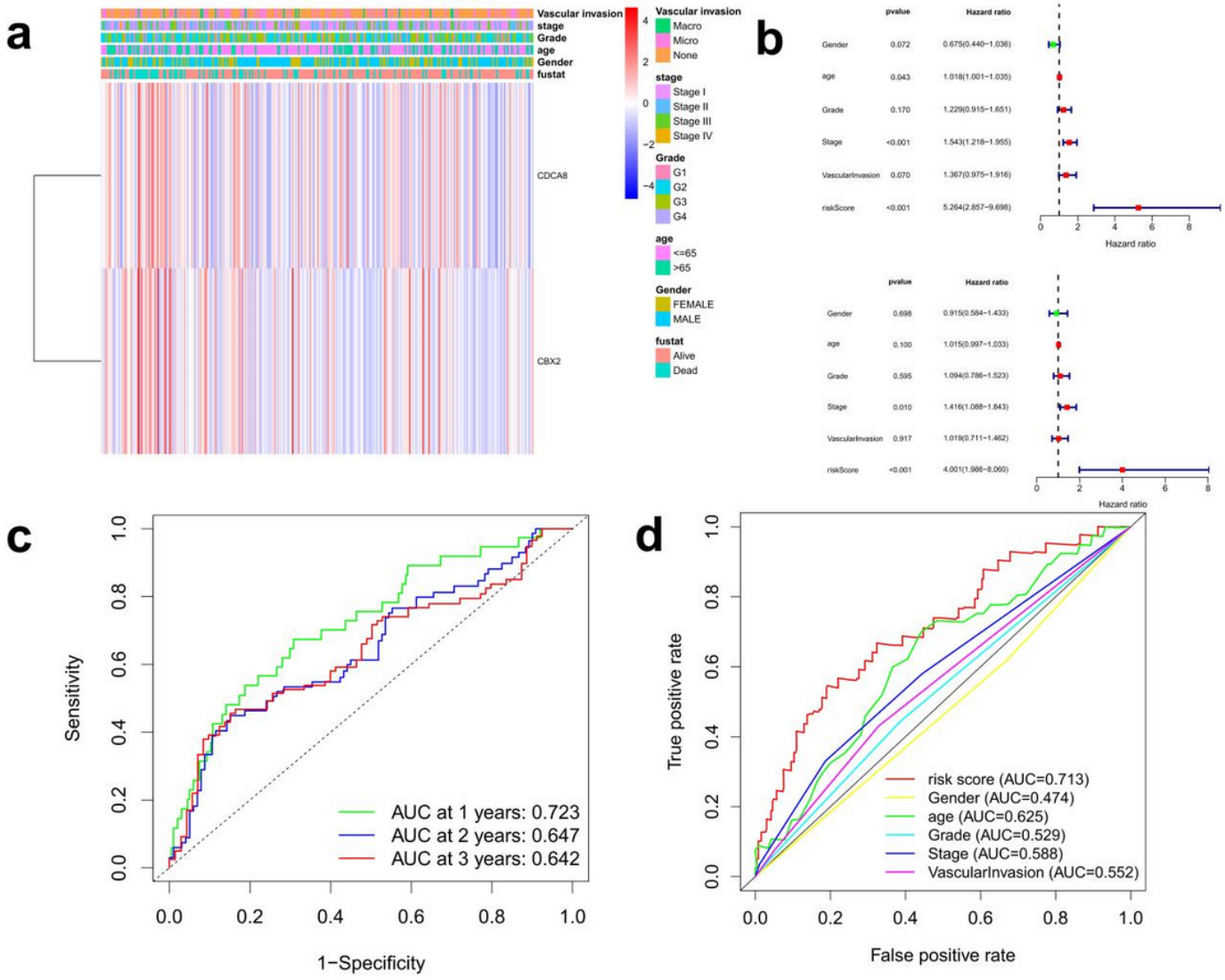

Figure 4

Evaluation of the Prognostic Value. (a) A heat-map of two model genes in five clinical indicators in TCGA; (b) prognostic effect analysis of risk score and clinical features in HCC with univariate and multivariate Cox regression analysis; (c) Time-dependent ROC curves for predicting 1-, 2-, and 3-year OS of TCGA cohort; (d) The ROC analysis of the risk score and other prognostic clinical features in HCC.

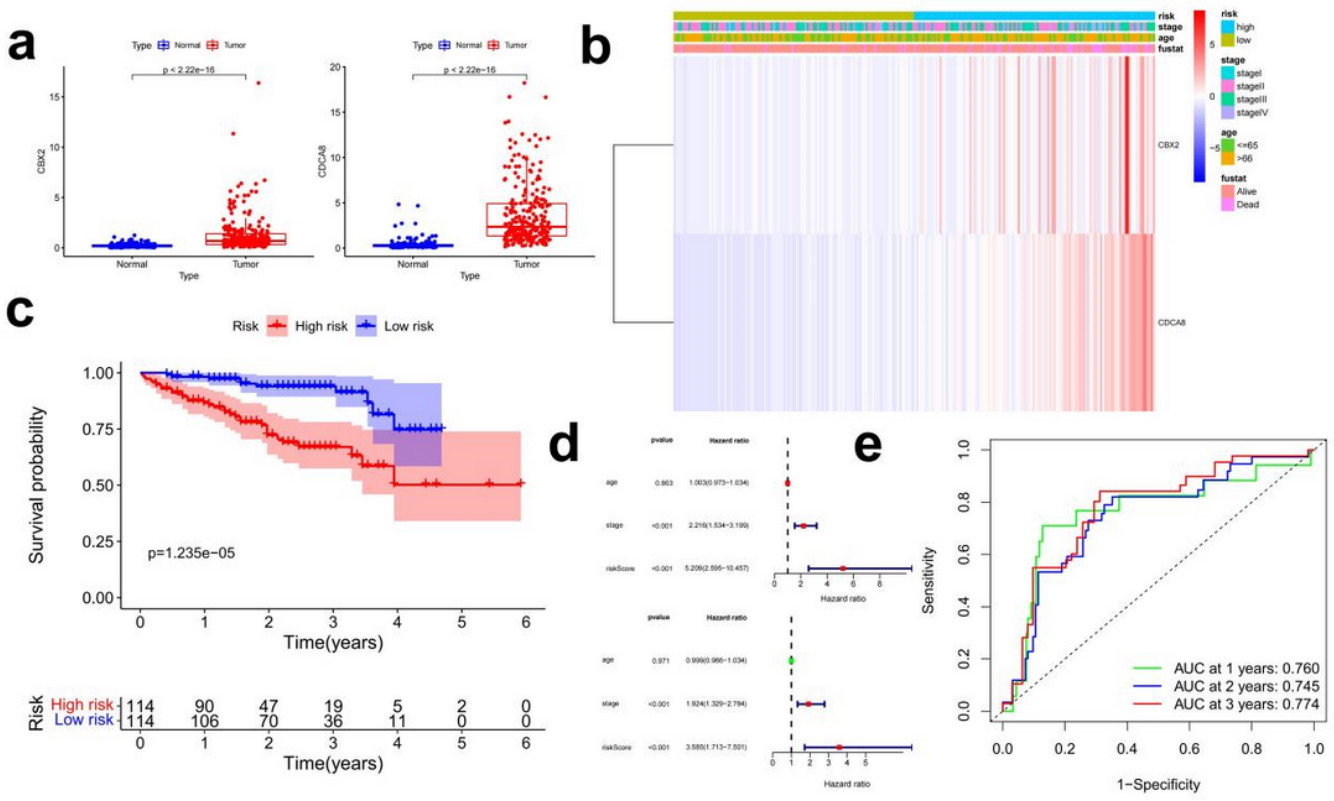

Figure 5

Validation of the prediction ability in the ICGC database. (a) The expression level of the two genes in the ICGC cohort; (b) The heat-map of two model gene and clinical characters in ICGC; (c) Kaplan–Meier analysis of the high- and low-risk groups among the HCC samples in the ICGC; (d) The univariate and multivariate Cox regression analysis of the risk score; (e) Time-dependent ROC curves for predicting 1-, 2-, and 3-year OS of ICGC cohort.

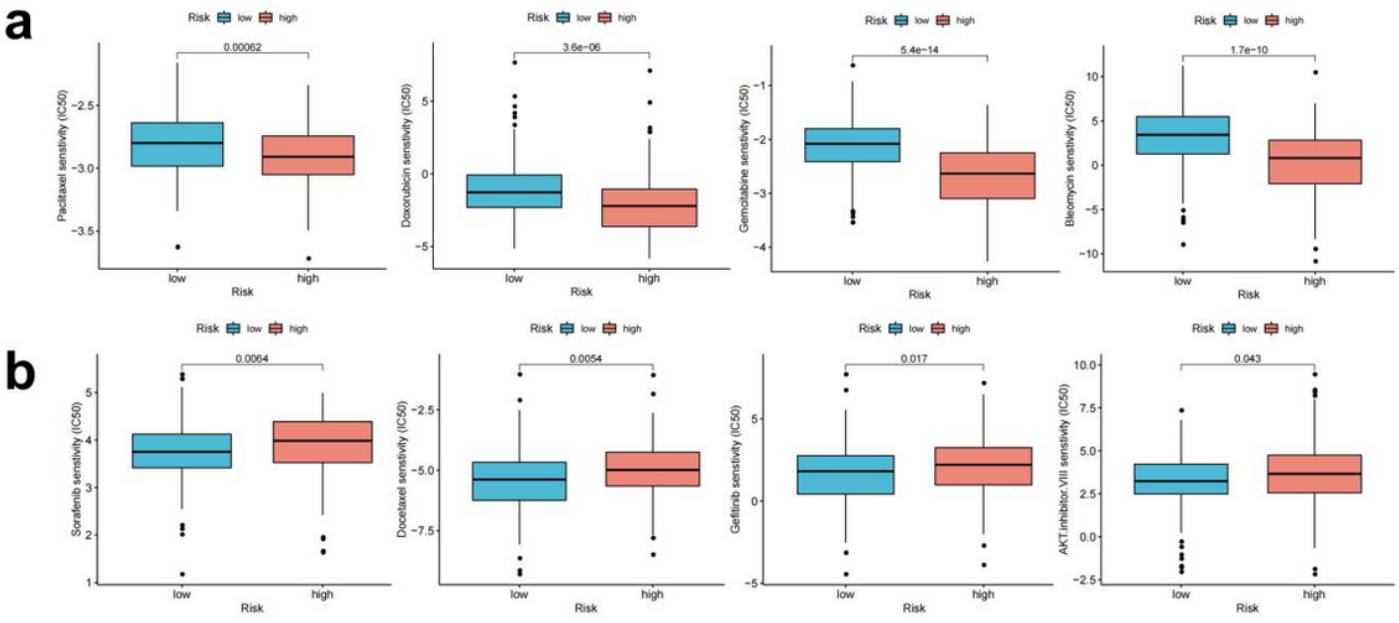

Figure 6

Sensitivity of the different risk groups to chemotherapy. (a) lower IC50 values in high-risk patients. (b) higher IC50 values in high-risk patients.

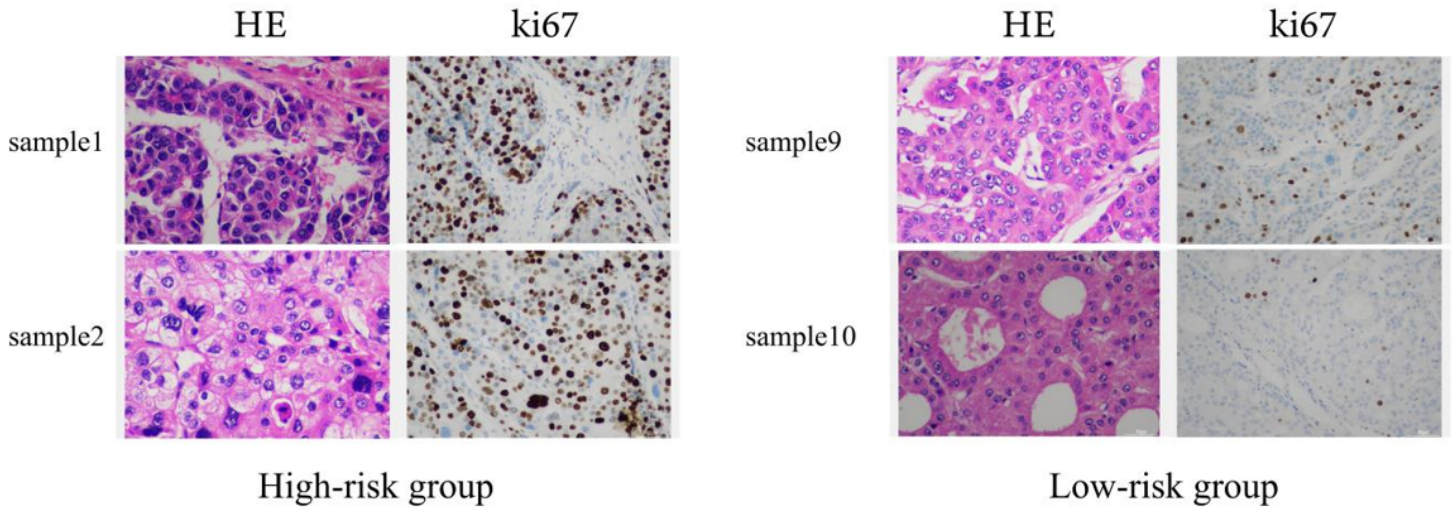

Figure 7

HE staining of clinical tumor tissues, and immunohistochemistry was used to detect the expression of Ki67 in HCC tissues.

Supplementary Files

This is a list of supplementary files associated with this preprint. Click to download.

- Supplementalfigure.docx